



Characterization of plaque phenotypes exhibiting an elevated pericoronary adipose tissue attenuation: insights from the REASSURE-NIRS registry

Satoshi Kitahara^{1,2,3} · Yu Kataoka³ · Hiroyuki Miura³ · Tatsuya Nishii⁴ · Kunihiro Nishimura⁵ · Kota Murai^{2,3} · Takamasa Iwai³ · Hideo Matama^{2,3} · Satoshi Honda³ · Masashi Fujino³ · Shuichi Yoneda³ · Kensuke Takagi³ · Fumiyuki Otsuka³ · Yasuhide Asaumi³ · Yusuke Fujino¹ · Kenichi Tsujita⁶ · Rishi Puri⁷ · Stephen J. Nicholls⁸ · Teruo Noguchi^{2,3}

Received: 11 December 2022 / Accepted: 19 June 2023 / Published online: 29 June 2023
© The Author(s) 2023

Abstract

Inflammation has been considered to promote atheroma instability. Coronary computed tomography angiography (CCTA) visualizes pericoronary adipose tissue (PCAT) attenuation, which reflects coronary artery inflammation. While PCAT attenuation has been reported to predict future coronary events, plaque phenotypes exhibiting high PCAT attenuation remains to be fully elucidated. The current study aims to characterize coronary atheroma with a greater vascular inflammation. We retrospectively analyzed culprit lesions in 69 CAD patients receiving PCI from the REASSURE-NIRS registry (NCT04864171). Culprit lesions were evaluated by both CCTA and near-infrared spectroscopy/intravascular ultrasound (NIRS/IVUS) imaging prior to PCI. PCAT attenuation at proximal RCA (PCAT_{RCA}) and NIRS/IVUS-derived plaque measures were compared in patients with PCAT_{RCA} attenuation \geq and $<$ -78.3 HU (median). Lesions with PCAT_{RCA} attenuation \geq -78.3 HU exhibited a greater frequency of maxLCBI_{4mm} \geq 400 (66% vs. 26%, $p < 0.01$), plaque burden \geq 70% (94% vs. 74%, $p = 0.02$) and spotty calcification (49% vs. 6%, $p < 0.01$). Whereas positive remodeling (63% vs. 41%, $p = 0.07$) did not differ between two groups. On multivariable analysis, maxLCBI_{4mm} \geq 400 (OR = 4.07; 95%CI 1.12–14.74, $p = 0.03$), plaque burden \geq 70% (OR = 7.87; 95%CI 1.01–61.26, $p = 0.04$), and spotty calcification (OR = 14.33; 95%CI 2.37–86.73, $p < 0.01$) independently predicted high PCAT_{RCA} attenuation. Of note, while the presence of only one plaque feature did not necessarily elevate PCAT_{RCA} attenuation ($p = 0.22$), lesions harboring two or more features were significantly associated with higher PCAT_{RCA} attenuation. More vulnerable plaque phenotypes were observed in patients with high PCAT_{RCA} attenuation. Our findings suggest PCAT_{RCA} attenuation as the presence of profound disease substrate, which potentially benefits from anti-inflammatory agents.

Keywords Lipid-rich plaque · Large plaque burden · Spotty calcification · Positive remodeling · Anti-inflammatory agents

✉ Yu Kataoka
yu.kataoka@ncvc.go.jp

¹ Department of Cardiology, Kashiwa Kousei General Hospital, 617 Shikoda, Kashiwa, Chiba 277-0862, Japan

² Department of Advanced Cardiovascular Medicine, Graduate School of Medical Sciences, Kumamoto University, 1-1-1 Chuo-Ku, Honjo, Kumamoto 860-8556, Japan

³ Department of Cardiovascular Medicine, National Cerebral & Cardiovascular Center, 6-1 Kishibe-Shimmachi, Suita, Osaka 564-8565, Japan

⁴ Department of Radiology, National Cerebral & Cardiovascular Center, 6-1 Kishibe-Shimmachi, Suita, Osaka 564-8565, Japan

⁵ Department of Preventive Medicine and Epidemiology, National Cerebral & Cardiovascular Center, 6-1 Kishibe-Shimmachi, Suita, Osaka 564-8565, Japan

⁶ Department of Cardiovascular Medicine, Graduate School of Medical Sciences, Kumamoto University, 1-1-1 Honjo, Chuo-Ku, Kumamoto 860-8556, Japan

⁷ Department of Cardiovascular Medicine, Cleveland Clinic, 9500 Euclid Avenue, Cleveland, OH 44195, USA

⁸ Victorian Heart Institute, Monash University, 631 Blackburn Rd, Clayton, VIC 3168, Australia

Abbreviations

AUC	Area under the curve
CAD	Coronary artery disease
CCTA	Coronary computed tomography angiography
DSCT	Dual-source CT
EEM	External elastic membrane
IVUS	Intravascular ultrasound
NIRS	Near-infrared spectroscopy
PCAT	Pericoronary adipose tissue
QCA	Quantitative coronary angiography
RCA	Right coronary artery
RI	Remodeling index
ROC	Receiver-operating characteristics

Introduction

Inflammation has been considered as an important driver which promotes atherosclerosis [1]. Recently, coronary computed tomography angiography (CCTA) has been shown to enable visualization of pericoronary adipose tissue (PCAT) attenuation, which reflects the degree of coronary artery inflammation [2–4]. Several observational studies reported the association of PCAT attenuation with future coronary events [5–7]. Pathophysiologically, coronary artery inflammation is recognized to induce the influx of lipidic materials into vessel wall [8, 9], leading to the formation of unstable plaque associated with future coronary events. However, it remains to be fully elucidated phenotypic features of coronary plaque presenting PCAT attenuation.

Near-infrared spectroscopy (NIRS) imaging quantitatively evaluates the degree of lipidic plaque materials *in vivo* [10]. This modality provides an opportunity to evaluate the association between *in vivo* coronary artery inflammation and lipidic plaque materials. Therefore, the current study sought to determine culprit plaque features in patients with coronary artery disease (CAD) associated with high coronary inflammation by analyzing both PCAT and NIRS imaging.

Methods

Study population

We retrospectively analyzed 111 consecutive patients with CAD who underwent both clinically indicated CCTA and NIRS/intravascular ultrasound (IVUS) imaging prior to percutaneous coronary intervention (PCI) (1 Aug. 2015 – 31 Dec. 2021) from the REASSURE-NIRS registry (REvelation of PATHophysiological PhenotypeS of VUIneRable Lipid-Rich Plaque on Near-InfraRed Spectroscopy) (NCT 04864171) (Supplementary Fig. 1). Of these, the following

subjects were excluded; those imaged by inadequate CCTA imaging protocol ($n = 17$), patients with poor quality of NIRS/IVUS images ($n = 1$), a case with in-stent restenosis lesion ($n = 1$), and the interval between CCTA and NIRS/IVUS imaging > 4 months ($n = 23$). As a consequence, the remaining 69 patients with 69 *de novo* target lesions were included into the current study analysis. Target lesion was defined as the segment receiving PCI. The median time from CCTA to PCI was 38 days. The study protocol conforms to the ethical guidelines of the 1975 Declaration of Helsinki, and it was approved by the institutional ethics committee (research project number: M30-084-6).

CCTA protocol

CCTA was performed by the second and third-generation dual-source CT (DSCT) scanners (SOMATOM Definition Flash and SOMATOM Force; Siemens Healthcare, Forchheim, Germany). Retrospective ECG-gated spiral scan with tube current modulation or prospective ECG triggered high-pitch spiral scan was selected depending on the heart rate. Further scan parameters in the second and third-generation DSCT were as follows: section collimation $2 \times 64 \times 0.6$ -mm and $2 \times 96 \times 0.6$ -mm, gantry rotation 0.275 s and 0.25 s, respectively. Automated tube current modulation (CARE Dose4D, Siemens) and automatic tube-voltage selection (CARE kV, Siemens) were used with 240–280 mAs as qualified reference tube-current time products and 120-kV as reference tube-voltage. The images were reconstructed using iterative reconstruction (SAFIRE or ADMIRE, Siemens) with 0.6-mm slice thickness and 0.3-mm increments with a medium convolution kernel (I31f or Bv40). The current CCTA imaging protocol was complied with the SCCT guidelines for performance of coronary computed tomographic angiography [11].

PCAT analysis

Semi-automated software (Aquarius 3D Workstation, TerraRecon Inc., San Mateo, CA, USA) was used to measure PCAT attenuation at the proximal right coronary artery ($PCAT_{RCA}$ attenuation) and at target lesion ($PCAT_{Lesion}$ attenuation), respectively. Analysis of $PCAT_{RCA}$ attenuation involved the proximal 10–50 mm of the RCA [2, 3, 12]. $PCAT_{Lesion}$ attenuation was measured at target lesions with the proximal and distal borders of the analysis region which were defined as the proximal and distal ends of the target lesion [2, 13, 14]. A centerline was applied to both the proximal segment of RCA and the target lesion, and then adventitia was demarcated from surrounding adipose tissue. Adipose tissue was defined as all voxels between -190 Hounsfield units (HU) and -30 HU within a pre-defined volume of interest. This volume interest included

three-dimensional concentric layers extending outward from the operator traced vessel wall to an extent of the reference diameter of the target lesion. PCAT attenuation was automatically quantified as the mean attenuation of all voxels within by the manually defined centerline and vessel wall. PCAT measurement was conducted by two independent experienced operators who were blinded to clinical data (SK, HM).

NIRS/IVUS imaging

NIRS/IVUS imaging was conducted prior to PCI to evaluate the entire target vessel. After intracoronary administration of nitroglycerin (100–300 µg), the imaging catheter (TVC Insight™ or Dualpro™, Infraredx, Bedford, MA, USA) was automatically pullbacked from the most distal site of the target artery at a speed of 0.5 mm/sec and 960 rpm (TVC Insight™) or 2.0 mm/sec and 1800 rpm (Dualpro™) [15]. Makoto® system (Infraredx, Bedford, MA, USA) was used to analyze obtained chemogram data [16]. MaxLCBI_{4mm} at target lesion was used for the analysis [17]. Qualitative analysis on IVUS imaging was performed to evaluate (1) plaque area, (2) remodeling index (RI), and (3) spotty calcification. Plaque area was defined as the difference in area occupied by the lumen and external elastic membrane (EEM) borders. Total atheroma volume was calculated by the summation of the plaque area in each measured image. Plaque burden was calculated as the percentage of total atheroma volume to EEM. RI was assessed in short axis view of the vessel by the following formula;

$$RI = (\text{cross-sectional EEM area at minimum lumen area}) / (\text{EEM area of the proximal reference segment}).$$

$RI \geq 1.05$ was considered as positive remodeling [18]. The presence of calcification was assessed at every 1-mm cross-sectional image, and then the arc of calcification was measured. Spotty calcification was defined as the presence of lesions 1 to 4 mm in length containing an arc of calcification $< 90^\circ$ [19]. NIRS/IVUS images were analyzed by physicians who were blinded to the clinical characteristics of the patients (KM and YK).

Quantitative coronary angiography analysis

Quantitative coronary angiography (QCA) analysis was performed at target and non-target lesions by using off-line commercially available software (QAngio® XA, Medis, Leiden, the Netherlands). QCA analysis included minimal lumen diameter, percent diameter stenosis, lesion length and reference vessel diameter.

Statistical analysis

Continuous variables were expressed as the mean \pm standard deviation and compared using the t test if data were normally distributed. Non-normally distributed continuous data were summarized as the median (interquartile range) and compared using the Wilcoxon rank sum test. Categorical variables were compared using the Fisher exact test or the Chi-square test as appropriate. Spearman's rank-order correlation was used to examine the relationship of PCAT_{RCA} attenuation with maxLCBI_{4mm}. Nominal logistic regression analysis was conducted to determine NIRS/IVUS plaque features associated with high PCAT_{RCA} attenuation. Parameters with P value < 0.10 in univariable analysis were entered into multivariable one. Receiver-operating characteristic (ROC) curve analyses were conducted to evaluate the ability of clinical features (age, sex, dyslipidemia and LDL-C ≥ 1.8 mmol/L) and PCAT_{RCA} for the prediction of NIRS/IVUS-derived vulnerable plaque [20, 21]. According to the published paper analyzing lipid (n = 40) and non-lipid (n = 15) plaques [22], the expected difference in the frequency of low attenuation plaque is considered as 10% between these two types of plaques. A sample of 56 lesions will be required for 90% power at a two-sided alpha level of 0.05 to detect a nominal difference of 10%, assuming a standard deviation of 10%. All P values < 0.05 were considered statistically significant. All analyses were performed with JMP version 14 (SAS Institute, Cary, NC).

Results

Clinical demographics of study subjects

The median PCAT_{RCA} attenuation was -78.3 HU. Study subjects were stratified into two groups according to the median PCAT_{RCA} attenuation. Baseline clinical characteristics of study population are summarized in Table 1. Patients were predominantly male (80%) with a high prevalence of hypertension (72%), dyslipidemia (86%) and type 2 diabetes mellitus (33%). Eighty-six percent of study subjects presented stable CAD. With regard to the use of anti-atherosclerotic medical therapies, 59% and 14% of study subjects received statin and ezetimibe, respectively. Lipids measures and c-reactive protein levels did not differ between two groups. (Table 1).

Coronary angiographic features of analyzed lesions

Table 2 shows characteristics of 69 analyzed lesions. Over two-thirds of analyzed lesions were located within the left anterior descending artery. There were no significant differences in QCA measures between two groups.

Table 1 Clinical Characteristics

	Total (n = 69)	PCAT _{RCA} attenuation ≥ -78.3HU (n = 35)	PCAT _{RCA} attenuation < -78.3HU (n = 34)	p value
Age, years	71 (55–77)	64 (52–77)	71 (61–76)	0.31
Male, n (%)	55 (80%)	28 (80%)	27 (79%)	0.95
BMI (kg/m ²)	23.9 (21.9–26.7)	24.1 (20.8–27.2)	23.9 (22.0–25.9)	0.74
Hypertension, n (%)	50 (72%)	24 (69%)	26 (76%)	0.46
Dyslipidemia, n (%)	59 (86%)	29 (83%)	30 (88%)	0.53
T2DM, n (%)	23 (33%)	12 (34%)	11 (32%)	0.86
Current Smoking, n (%)	12 (17%)	5 (14%)	7 (21%)	0.49
Prior PCI, n (%)	25 (36%)	13 (37%)	12 (35%)	0.87
Diagnosis of CAD				
Stable CAD, n (%)	59 (86%)	31 (89%)	28 (82%)	0.46
ACS, n (%)	10 (14%)	4 (11%)	6 (18%)	
Medication use				
Aspirin, n (%)	19 (28%)	13 (37%)	6 (18%)	0.07
P2Y12 inhibitor, n (%)	10 (14%)	8 (23%)	2 (6%)	0.05
Statin, n (%)	41 (59%)	21 (60%)	20 (59%)	0.92
Ezetimibe, n (%)	10 (14%)	4 (11%)	6 (18%)	0.46
β-blocker, n (%)	26 (38%)	15 (43%)	11 (32%)	0.37
ACE-I / ARB, n (%)	29 (42%)	9 (26%)	20 (59%)	0.01
Laboratory data				
eGFR (mL/min/1.73m ²)	66 (60–73)	69 (61–83)	63 (59–70)	0.06
LDL-C (mmol/l)	2.59 (2.09–3.41)	2.56 (2.07–3.28)	2.61 (1.93–3.41)	0.65
HDL-C (mmol/l)	1.24 (1.06–1.42)	1.29 (1.14–1.42)	1.11 (1.03–1.47)	0.42
Triglyceride (mmol/l)	1.29 (0.90–1.98)	1.06 (0.88–1.69)	1.46 (0.95–2.13)	0.11
HbA1c (%)	5.8 (5.6–6.5)	5.9 (5.6–6.4)	5.8 (5.6–6.4)	0.83
CRP (μg/l)	900 (300–2100)	500 (200–1800)	1100 (500–2200)	0.50

Non-normally distributed continuous data were summarized as the median (interquartile range)

ACE-I= angiotensin converting enzyme inhibitor, ACS= acute coronary syndrome, ARB= angiotensin II receptor blocker, BMI= body mass index, CAD= coronary artery disease, eGFR= estimated glomerular filtration rate, HDL= high density lipoprotein, LAD= left anterior descending artery, LDL= low density lipoprotein, PCAT= pericoronary adipose tissue, PCI= percutaneous coronary intervention, RCA= right coronary artery, T2DM= Type2 diabetes mellitus

Characteristics of PCAT and NIRS/IVUS measures

On PCAT analysis, lesions with PCAT_{RCA} attenuation ≥ -78.3 HU exhibited a higher PCAT_{Lesion} attenuation. NIRS/IVUS imaging analysis demonstrated a greater maxLCBI_{4mm} (466 ± 210 vs. 338 ± 211, p = 0.01) at lesions with PCAT_{RCA} attenuation ≥ -78.3 HU, accompanied by a higher frequency of maxLCBI_{4mm} ≥ 400 (66% vs. 26%, p < 0.01) (Table 2). In addition, a greater plaque burden, a higher proportion of plaque burden ≥ 70% and spotty calcification were observed at lesions with PCAT_{RCA} attenuation ≥ -78.3 HU. There was a trend toward a greater remodeling index and a higher frequency of positive remodeling in those with PCAT_{RCA} attenuation ≥ -78.3 HU, but these comparisons did not meet statistical significance (Table 2).

Figure 1 illustrated the relationships of PCAT_{RCA} attenuation with maxLCBI_{4mm}, plaque burden and remodeling index, respectively. MaxLCBI_{4mm} (R = 0.37, p < 0.01, Fig. 1A), plaque burden (R = 0.35, p < 0.01, Fig. 1B) and remodeling index (R = 0.25, p = 0.04, Fig. 1C) were positively associated with PCAT_{RCA} attenuation.

With regards to PCAT_{Lesion}, PCAT_{Lesion} attenuation were significantly correlated with PCAT_{RCA} attenuation (R = 0.70, p < 0.01) (Supplementary Fig. 2) and plaque burden (R = 0.29, p = 0.01), respectively. However, the relationships of PCAT_{Lesion} attenuation with maxLCBI_{4mm} (R = 0.23, p = 0.05) and remodeling index (R = 0.16, p = 0.20) were not statistically significant (Supplementary Fig. 3 a-c). Furthermore, PCAT_{Lesion} attenuation did not

Table 2 Angiographical and imaging analysis

	Total (n = 69)	PCAT _{RCA} attenuation ≥ -78.3HU (n = 35)	PCAT _{RCA} attenuation < -78.3HU (n = 34)	P value
Culprit lesion				
LMT, n (%)	4 (6%)	3 (9%)	1 (3%)	
LAD, n (%)	46 (67%)	22 (63%)	24 (71%)	
LCX, n (%)	6 (9%)	3 (9%)	3 (9%)	
RCA, n (%)	13 (19%)	7 (20%)	6 (18%)	
Proximal segment, n (%)	41 (59%)	23 (66%)	18 (53%)	0.28
QCA analysis				
%Diameter stenosis (%)	68.0 ± 16.5	67.5 ± 17.2	68.5 ± 15.9	0.56
Lesion length (mm)	19.0 (13.6–22.9)	17.8 (12.9–21.2)	19.8 (14.2–23.8)	0.81
Reference diameter (mm)	3.5 ± 0.7	3.6 ± 0.6	3.5 ± 0.8	0.47
PCAT analysis				
PCAT _{RCA} attenuation (HU)	- 78.3 (- -86.3 to - 71.7)	- 71.9 (- 76.0 to - 69.2)	- 86.3 (- 91.3 to - 82.1)	< 0.01
PCAT _{Lesion} attenuation (HU)	- 79.3 ± 12.2	- 72.4 ± 9.4	- 86.5 ± 10.6	< 0.01
NIRS measurement				
MaxLCBI _{4mm}	403 ± 219	466 ± 210	338 ± 211	0.01
MaxLCBI _{4mm} ≥ 400, n (%)	32 (46%)	23 (66%)	9 (26%)	< 0.01
IVUS measurement				
Plaque burden (%)	59 (54–64)	61 (58–65)	56 (47–62)	< 0.01
Plaque burden ≥ 70%, n (%)	58 (84%)	33 (94%)	25 (74%)	0.02
Remodeling index	1.07 (0.97–1.28)	1.15 (0.98–1.29)	1.02 (0.97–1.17)	0.10
Remodeling index ≥ 1.05, n (%)	36 (52%)	22 (63%)	14 (41%)	0.07
Spotty calcification, n (%)	19 (28%)	17 (49%)	2 (6%)	< 0.01

Continuous data are represented as means ± standard deviation if data were normally distributed Non-normally distributed continuous data were summarized as the median (interquartile range)

IVUS= intravascular ultrasound, LAD= left anterior descending artery, LCX= left circumflex artery, LMT= left main trunk, MaxLCBI_{4mm}= maximum 4 mm Lipid Core Burden Index, NIRS= near-infrared spectroscopy, PCAT= pericoronary adipose tissue, RCA= right coronary artery, QCA= quantitative coronary angiography

Significant P value < 0.05 is indicated in bold

differ between lesions with and without spotty calcification (Supplementary Fig. 4).

Factors associated with high PCAT_{RCA} attenuation

Uni- and multivariable logistic regression analyses were conducted to identify an independent NIRS/IVUS-derived feature associated with PCAT_{RCA} attenuation ≥ -78.3 HU. Univariable analysis revealed that maxLCBI_{4mm} ≥ 400, maximum plaque burden ≥ 70% and the presence of spotty calcification were associated with high PCAT_{RCA} attenuation (Table 3). On multivariable analysis, these plaque measures emerged as the independent predictors of PCAT_{RCA} attenuation ≥ - 8.3 HU (maxLCBI_{4mm} ≥ 400: OR = 4.07, 95%CI 1.12–14.74, p = 0.03, maximal plaque burden ≥ 70%: OR = 7.87, 95%CI 1.01–61.26, p = 0.04, spotty calcification:

OR = 14.33, 95%CI 2.37–86.73, p < 0.01, Table 3) but not positive remodeling (OR = 1.26, 95%CI 0.36–4.45, p = 0.72).

PCAT_{RCA} attenuation was compared in lesions stratified according to the number of NIRS/IVUS-derived features (Fig. 2). PCAT_{RCA} attenuation at lesions with one NIRS/IVUS-derived plaque feature was similar to that at lesions without any plaque features (p = 0.22). By contrast, PCAT_{RCA} attenuation was greater in association with an increasing number of plaque features (Fig. 2). ROC curve analyses were conducted to evaluate the ability of PCAT_{RCA} for the prediction of NIRS/IVUS-derived vulnerable plaque (Fig. 3). PCAT_{RCA} exhibited an excellent predictive ability of vulnerable plaque [area under the curve (AUC) = 0.82, p < 0.01]. Furthermore, the addition of PCAT_{RCA} with clinical features (age, sex, dyslipidemia and LDL-C ≥ 1.8 mmol/L) improved its prediction [model 1 (age, sex and dyslipidemia): AUC = 0.69, model 2 (age, sex, dyslipidemia and

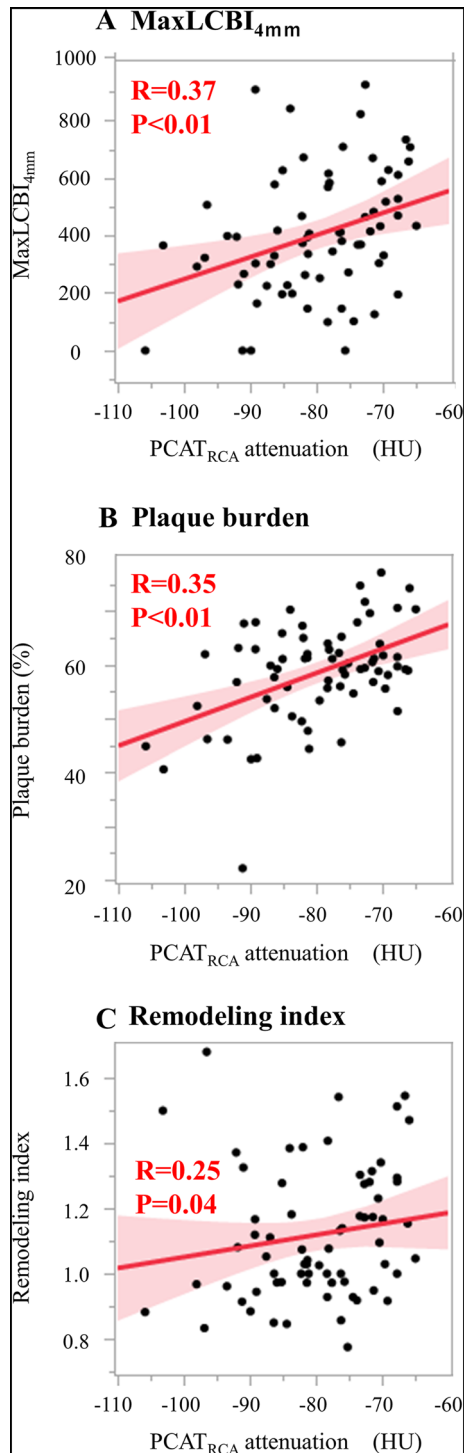


Fig. 1 The correlation between NIRS/IVUS-derived plaque features and PCAT_{RCA} attenuation. **A** MaxLCBI_{4mm}, **B** Plaque burden, **C** Remodeling index. IVUS= intravascular ultrasound, NIRS= near infrared spectroscopy, PCAT= pericoronary adipose tissue, maxLCBI_{4mm} = maximum-4 mm lipid core burden index, RCA= right coronary artery

LDL-C ≥ 1.8 mmol/L): AUC = 0.70, model 3 (age, sex, dyslipidemia, LDL-C ≥ 1.8 mmol/L and PCAT_{RCA} attenuation ≥ -78.3 HU): AUC = 0.89] (Fig. 3). Two representative cases are shown in Fig. 4.

Discussion

While evaluation of coronary artery inflammation has a potential to stratify future risks of coronary events [1], whether this approach truly reflects disease substrate associated with the occurrence of coronary events remains to be fully determined yet. In the current study, patients with a higher CCTA-derived PCAT_{RCA} attenuation exhibited a greater atheroma burden at target lesions. Furthermore, accumulation of lipidic plaque component and spotty calcification were more frequently observed in patients with a higher PCAT_{RCA} attenuation. These findings highlight the ability of PCAT_{RCA} attenuation to non-invasively identify high-risk plaque phenotypes causing future coronary events.

Pericoronary adipose tissue has been recently recognized as an important contributor to atherosclerosis via secreting proinflammatory adipokines and cytokines. Pathophysiologically, proinflammatory stimuli secreted from pericoronary adipose tissue diffusely propagate into the adventitia, media, and intima. These properties interact with endothelial cells and vascular smooth muscle cells, which cause the formation, progression and destabilization of atherosclerotic plaques [23, 24]. In particular, inflammatory activities could promote the influx of lipidic materials within vessel wall [8, 9]. In the current study, in addition to plaque area, maxLCBI_{4mm} at target lesions increased in association with PCAT_{RCA} attenuation in vivo. One recent study characterized coronary atherosclerosis as the concomitance of macrophage polarization with a greater expression of interleukin-6, tumor necrosis factor-alpha and monocyte chemoattractant protein-1 [25]. Our findings as well as the aforementioned study suggest in vivo relationship of inflammatory activity at pericoronary adipose tissue with the formation of lipidic coronary atheroma in patients with CAD.

Spotty calcification is a phenotypic feature of coronary atheroma which reflects active form of disease stimulated by inflammation. Mechanistically, inflammatory cytokines such as tumor necrosis factor-alpha activate osteogenic differentiation and mineralization of vascular cells, which contribute to early stages of plaque calcification [26, 27]. The current analysis observed an increased frequency of spotty calcification in patients with high PCAT_{RCA} attenuation. This finding suggests that patients with vascular inflammation may exhibit a greater degree of plaque inflammation, which could promote its instability and then cause future coronary events. Intravascular imaging studies showed an accelerated progression and more unstable features at spotty calcified

Table 3 Uni- and multivariable analysis for detecting high PCAT_{RCA} attenuation

	Univariable analysis			Multivariable analysis*		
	OR	95%CI	P value	OR	95%CI	P value
Age	0.97	0.93–1.01	0.15	0.99	0.94–1.05	0.72
Male	1.04	0.32–3.35	0.95	1.05	0.23–4.71	0.95
Hypertension	0.67	0.23–1.95	0.46			
Dyslipidemia	0.64	0.16–2.52	0.53			
Diabetes mellitus	1.09	0.40–2.97	0.86			
Statin use	1.05	0.40–2.74	0.92			
LDL-C	1.00	0.99–1.01	1.00			
MaxLCBI _{4mm} ≥ 400	5.32	1.89–14.96	<0.01	4.07	1.12–14.74	0.03
Maximal plaque burden ≥ 70%	5.94	1.18–29.95	0.03	7.87	1.01–61.26	0.049
Positive remodeling†	2.42	0.92–6.36	0.07	1.26	0.36–4.45	0.72
Spotty calcification	15.11	3.13–72.99	<0.01	14.33	2.37–86.73	<0.01

CI= Confidence interval, LDL= low density lipoprotein, MaxLCBI_{4mm}= maximum-4 mm Lipid Core Burden Index, OR= Odds ratio, PCAT= pericoronary adipose tissue, RCA= right coronary artery

†Positive remodeling was defined as remodeling index ≥ 1.05

*Multivariable logistic regression analysis with factors that were significant in the univariable analysis (p value <0.10), age, and male

Significant P value <0.05 is indicated in bold

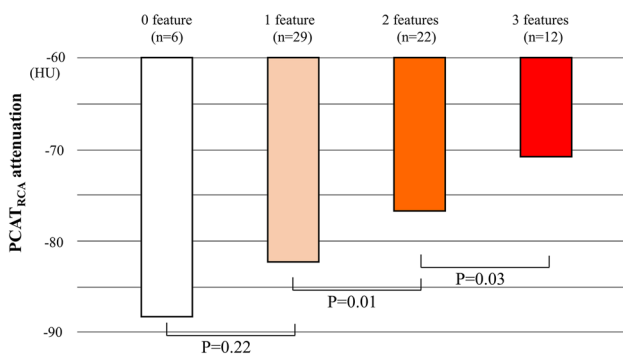
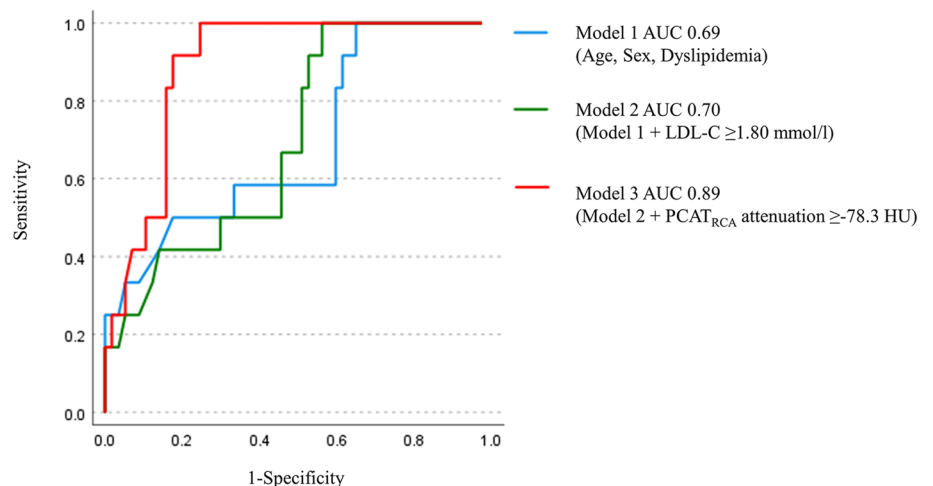


Fig. 2 The median PCAT_{RCA} attenuation and the number of NIRS/IVUS-derived plaque features. IVUS= intravascular ultrasound, NIRS= near infrared spectroscopy, PCAT= pericoronary adipose tissue, RCA= right coronary artery

Fig. 3 Receiver operating characteristics curve analysis to predict vulnerable plaques. Three models were used to evaluate the predictive ability of NIRS/IVUS-derived vulnerable plaque (= maxLCBI_{4mm} > 400 + plaque burden > 70% + spotty calcification). Model 1: age, sex, and dyslipidemia (light blue). Model 2: model 1 + LDL-C ≥ 1.8 mmol/L (green). Model 3: model 2 + PCAT_{RCA} attenuation ≥ -78.3 HU (red)



lesions [28]. These observations support evaluation of PCAT_{RCA} attenuation as a tool to measure plaque inflammation associated with its progression/rupture.

The current study underscores a clustering of phenotypic plaque features in patients exhibiting an elevated vascular inflammation. As shown in Fig. 2, PCAT_{RCA} attenuation did not increase even if one plaque feature existed, whereas clustering of more than two features associates with a higher level of PCAT_{RCA} attenuation. The cardiovascular effects of clustering plaque features have been reported by the PROSPECT study [29]. In this study, cardiovascular events' risks incrementally elevate in association with the number of plaque features including its volume and thin-cap fibroatheroma. Another study elucidated substantially progressive disease substrate in

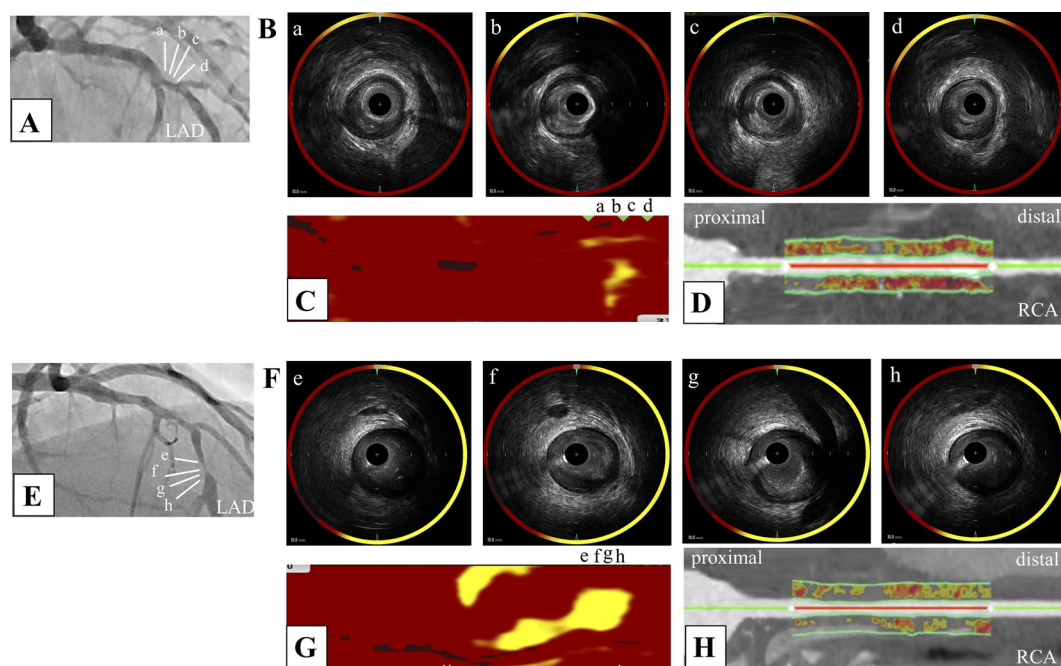


Fig. 4 Representative cases with or without high vascular inflammation. **A** 77 years old male with stable coronary artery disease. Coronary angiography demonstrated that moderate stenosis in his middle left descending artery (LAD). **B** Grey-scale intravascular ultrasound (IVUS) showed calcified plaque with no attenuation in the culprit lesion. **C** Near-infrared spectroscopy chemogram revealed that there was less lipid accumulation in the culprit lesion ($\text{maxLCBI}_{4\text{mm}}=292$). **D** In coronary computed tomography angiography (CCTA) analysis, his pericoronary adipose tissue attenua-

tion at proximal RCA was low (PCAT_{RCA} attenuation = -98.1 HU). **E** 85 years old male with stable coronary artery disease. Coronary angiography demonstrated that severe stenosis in his middle LAD. **F** Grey-scale IVUS showed low echoic plaque with attenuation in the culprit lesion. **G** NIRS chemogram revealed that there was large lipid burden in the culprit lesion ($\text{maxLCBI}_{4\text{mm}}=465$). **H** In CCTA analysis, he had high coronary artery inflammation (PCAT_{RCA} attenuation = -72.7 HU)

patients with multiple vulnerable plaque characteristics [30]. These observations provide mechanistic insights into the potential effect of vascular inflammation to induce the accumulation of multiple atherosclerotic features, which account for the predictive ability of PCAT_{RCA} attenuation to predict future risk of cardiovascular events.

The current study used PCAT_{RCA} attenuation as a marker reflecting inflammation of the entire coronary tree, whereas $\text{PCAT}_{\text{Lesion}}$ may be better to evaluate lesion-related inflammation activity. In our analysis, while $\text{PCAT}_{\text{Lesion}}$ was attenuation positively correlated with PCAT_{RCA} attenuation ($R=0.70$, $p<0.01$), the correlation of $\text{PCAT}_{\text{Lesion}}$ attenuation with NIRS/IVUS-derived plaque features were weak. Most of published studies have measured PCAT attenuation at the proximal 40 mm segment of RCA, and they reported that PCAT_{RCA} predicted a future cardiovascular event [7]. This measurement of PCAT is based on pathophysiological and anatomical features of RCA. Adipose tissues abundantly exist at the proximal segment of RCA, which could better reflect inflammatory activity [2]. In addition, the number of side branches at this segment is low, and luminal diameter does not dynamically change throughout the proximal segment of RCA [3]. These anatomical characteristics

are suitable to clearly visualize PCAT attenuation. In our study, $\text{maxLCBI}_{4\text{mm}}$ was associated with PCAT_{RCA} but not $\text{PCAT}_{\text{Lesion}}$ attenuation. Our observation also supports the measurement of PCAT attenuation at the proximal segment of RCA to more appropriately evaluate coronary artery inflammation.

To date, clinically adequate cut-off value of PCAT_{RCA} attenuation is not fully established yet. Tzolos et al. reported that PCAT_{RCA} attenuation ≥ -70.5 HU predicted future outcome [6], whereas other study showed its value ≥ -76.3 HU as a contributor for outcomes [7]. In the current study, we used the median value of PCAT_{RCA} attenuation in the entire subjects (-78.3 HU) as a cut-off value of PCAT_{RCA} attenuation. Further studies are required to identify the best cut-off value of PCAT_{RCA} attenuation associated with plaque instability and cardiovascular outcomes.

Considerable interests have recently focused on inflammation as a therapeutic target because of its biological properties. The CANTOS (Canakinumab Antiinflammatory Thrombosis Outcome Study) study demonstrated the clinical benefit of modulating interleukin-1 β to reduce future atherosclerotic cardiovascular disease in patients with an elevated level of high-sensitivity c-reactive protein [31]. A significant

reduction of cardiovascular events in patients with recent myocardial infarction receiving colchicine has been reported by COLCOT (Colchicine Cardiovascular Outcomes Trial) study [32]. These evidence indicates that patients with elevated inflammatory activity may benefit from anti-inflammatory agents. Given that PCAT imaging is a non-invasive modality to evaluate inflammation activity, this approach may be clinically applicable to identify those who require anti-inflammatory therapies. Future dedicated studies will be warranted to elucidate whether PCAT-guided anti-inflammatory therapy could improve cardiovascular outcomes.

Several caveats should be noted. Firstly, this study is a single-center retrospective observational study. Secondly, the sample size of the current study is relatively small, which may lead to the wide 95% CI in the multivariable analysis. However, our calculation of study sample size shows that 56 lesions provide 90% power at a two-sided alpha level of 0.05 to detect a nominal difference of 10% (standard deviation = 10%). Thirdly, CCTA imaging was used according to each physician's discretion. These may cause a potential bias to select study population. Fourthly, the use of lipid-lowering therapy and its intensity were decided by each physician. Fifthly, while one recent study showed the association of PCAT_{RCA} attenuation with monocyte chemoattractant protein-1 and interleukin-7 [31], the current study did not measure inflammatory biomarkers.

In conclusion, patients with an elevated PCAT_{RCA} attenuation more likely exhibited greater atheroma burden containing lipidic materials and spotty calcification. Of note, a higher PCAT_{RCA} attenuation was observed in association with an increased number of these phenotypic features. Our findings suggest that CCTA-derived PCAT_{RCA} attenuation has a potential to non-invasively identify patients harboring high-risk plaque phenotype who may require preventive medical therapies including anti-inflammation agent.

Supplementary Information The online version contains supplementary material available at <https://doi.org/10.1007/s10554-023-02907-w>.

Acknowledgements We would like to acknowledge cardiology medical fellows and co-medical staffs (Sayaka Watanabe, Shintaro Kobayashi and Tomoyu Kondo) for their support to conduct NIRS/IVUS imaging during PCI. We thank Miss Yuko Yoshioka and Miss Emi Kanai for their excellent assistance.

Author contributions SK, HM and YK were responsible for the study design and concept. TN and TI collected the patient data. KM, HM, SH, MF, SY, KT, FO and YA performed the data cleaning. SK and KN performed the data analysis. SK and YK wrote the first draft of the manuscript with support from YF, RP, SN, KT, and TN supervised the project. All authors commented on previous version of the manuscript. All authors read and approved the final manuscript.

Funding This work was supported by Fukuda Foundation for Medical Technology.

Declarations

Conflict of interest The authors declare the following financial interests/personal relationships which may be considered as potential competing interests: Yu Kataoka has received research support from Nipro and Abbott, and honoraria from Nipro, Abbott, Kowa, Amgen, Sanofi, Astellas, Takeda and Daiichi-Sankyo. Other authors have nothing to disclose.

Ethical approval This study was performed in line with the principles of the Declaration of Helsinki. Approval was granted by the Ethics Committee of National Cerebral and Cardiovascular Center (research project number: M30-084-6).

Open Access This article is licensed under a Creative Commons Attribution 4.0 International License, which permits use, sharing, adaptation, distribution and reproduction in any medium or format, as long as you give appropriate credit to the original author(s) and the source, provide a link to the Creative Commons licence, and indicate if changes were made. The images or other third party material in this article are included in the article's Creative Commons licence, unless indicated otherwise in a credit line to the material. If material is not included in the article's Creative Commons licence and your intended use is not permitted by statutory regulation or exceeds the permitted use, you will need to obtain permission directly from the copyright holder. To view a copy of this licence, visit <http://creativecommons.org/licenses/by/4.0/>.

References

- Ross R (1999) Atherosclerosis—an inflammatory disease. *N Engl J Med* 340(2):115–126. <https://doi.org/10.1056/nejm199901143400207>
- Antonopoulos AS, Sanna F, Sabharwal N, Thomas S, Oikonomou EK et al (2017) Detecting human coronary inflammation by imaging perivascular fat. *Sci Transl Med*. <https://doi.org/10.1126/scitranslmed.aal2658>
- Oikonomou EK, Marwan M, Desai MY, Mancio J, Alashi A et al (2018) Non-invasive detection of coronary inflammation using computed tomography and prediction of residual cardiovascular risk (the CRISP CT study): a post-hoc analysis of prospective outcome data. *Lancet* 392(10151):929–939. [https://doi.org/10.1016/s0140-6736\(18\)31114-0](https://doi.org/10.1016/s0140-6736(18)31114-0)
- Lin A, Nerlekar N, Munnur RK, Kataoka Y, Andrews J et al (2020) Cholesterol crystal-induced coronary inflammation: Insights from optical coherence tomography and pericoronary adipose tissue computed tomography attenuation. *J Cardiovasc Comput Tomogr* 14(3):277–278. <https://doi.org/10.1016/j.jcct.2019.11.011>
- Yuvaraj J, Lin A, Nerlekar N, Munnur RK, Cameron JD et al (2021) Pericoronary adipose tissue attenuation is associated with high-risk plaque and subsequent acute coronary syndrome in patients with stable coronary artery disease. *Cells*. <https://doi.org/10.3390/cells10051143>
- Tzolos E, Williams MC, McElhinney P, Lin A, Grodecki K et al (2022) Pericoronary adipose tissue attenuation, low-attenuation plaque burden, and 5-year risk of myocardial infarction. *JACC Cardiovasc Imaging*. <https://doi.org/10.1016/j.jcmg.2022.02.004>
- van Diemen PA, Bom MJ, Driessen RS, Schumacher SP, Everaars H et al (2021) Prognostic value of RCA pericoronary adipose tissue CT-attenuation beyond high-risk plaques, plaque volume, and ischemia. *JACC Cardiovasc Imaging* 14(8):1598–1610. <https://doi.org/10.1016/j.jcmg.2021.02.026>

8. Hansson GK (2005) Inflammation, atherosclerosis, and coronary artery disease. *N Engl J Med* 352(16):1685–1695. <https://doi.org/10.1056/NEJMra043430>
9. Falk E (2006) Pathogenesis of atherosclerosis. *J Am Coll Cardiol* 47(8 Suppl):C7-12. <https://doi.org/10.1016/j.jacc.2005.09.068>
10. Wang J, Geng YJ, Guo B, Klima T, Lal BN et al (2002) Near-infrared spectroscopic characterization of human advanced atherosclerotic plaques. *J Am Coll Cardiol* 39(8):1305–1313. [https://doi.org/10.1016/s0735-1097\(02\)01767-9](https://doi.org/10.1016/s0735-1097(02)01767-9)
11. Abbata S, Blanke P, Maroules CD, Cheezum M, Choi AD et al (2016) SCCT guidelines for the performance and acquisition of coronary computed tomographic angiography: a report of the society of cardiovascular computed tomography guidelines committee: endorsed by the north american society for cardiovascular imaging (NASCI). *J Cardiovasc Comput Tomogr* 10(6):435–449. <https://doi.org/10.1016/j.jcct.2016.10.002>
12. Goeller M, Tamarappoo BK, Kwan AC, Cadet S, Commandeur F et al (2019) Relationship between changes in pericoronary adipose tissue attenuation and coronary plaque burden quantified from coronary computed tomography angiography. *Eur Heart J Cardiovasc Imaging* 20(6):636–643. <https://doi.org/10.1093/ehjci/jez013>
13. Goeller M, Achenbach S, Cadet S, Kwan AC, Commandeur F et al (2018) Pericoronary adipose tissue computed tomography attenuation and high-risk plaque characteristics in acute coronary syndrome compared with stable coronary artery disease. *JAMA Cardiol* 3(9):858–863. <https://doi.org/10.1001/jamacardio.2018.1997>
14. Kwiecinski J, Dey D, Cadet S, Lee SE, Otaki Y et al (2019) Pericoronary adipose tissue density is associated with (18)F-Sodium fluoride coronary uptake in stable patients with high-risk plaques. *JACC Cardiovasc Imaging* 12(10):2000–2010. <https://doi.org/10.1016/j.jcmg.2018.11.032>
15. Kataoka Y, Puri R, Andrews J, Honda S, Nishihira K et al (2017) In vivo visualization of lipid coronary atheroma with intravascular near-infrared spectroscopy. *Expert Rev Cardiovasc Ther* 15(10):775–785. <https://doi.org/10.1080/14779072.2017.1367287>
16. Gardner CM, Tan H, Hull EL, Lissauskas JB, Sum ST et al (2008) Detection of lipid core coronary plaques in autopsy specimens with a novel catheter-based near-infrared spectroscopy system. *JACC Cardiovasc Imaging* 1(5):638–648. <https://doi.org/10.1016/j.jcmg.2008.06.001>
17. Maddar RD, Goldstein JA, Madden SP, Puri R, Wolski K et al (2013) Detection by near-infrared spectroscopy of large lipid core plaques at culprit sites in patients with acute ST-segment elevation myocardial infarction. *JACC Cardiovasc Interv* 6(8):838–846. <https://doi.org/10.1016/j.jcin.2013.04.012>
18. Kume T, Okura H, Kawamoto T, Akasaka T, Toyota E et al (2008) Relationship between coronary remodeling and plaque characterization in patients without clinical evidence of coronary artery disease. *Atherosclerosis* 197(2):799–805. <https://doi.org/10.1016/j.atherosclerosis.2007.07.028>
19. Ehara S, Kobayashi Y, Yoshiyama M, Shimada K, Shimada Y et al (2004) Spotty calcification typifies the culprit plaque in patients with acute myocardial infarction: an intravascular ultrasound study. *Circulation* 110(22):3424–3429. <https://doi.org/10.1161/01.Cir.0000148131.41425.E9>
20. Nakamura H, Kataoka Y, Nicholls SJ, Puri R, Kitahara S et al (2022) Elevated Lipoprotein(a) as a potential residual risk factor associated with lipid-rich coronary atheroma in patients with type 2 diabetes and coronary artery disease on statin treatment: Insights from the REASSURE-NIRS registry. *Atherosclerosis* 349:183–189. <https://doi.org/10.1016/j.atherosclerosis.2022.03.033>
21. de Boer SP, Brugaletta S, Garcia-Garcia HM, Simsek C, Heo JH et al (2014) Determinants of high cardiovascular risk in relation to plaque-composition of a non-culprit coronary segment visualized by near-infrared spectroscopy in patients undergoing percutaneous coronary intervention. *Eur Heart J* 35(5):282–289. <https://doi.org/10.1093/eurheartj/ehj378>
22. Marwan M, Taher MA, El Meniawy K, Awadallah H, Pflederer T et al (2011) In vivo CT detection of lipid-rich coronary artery atherosclerotic plaques using quantitative histogram analysis: a head to head comparison with IVUS. *Atherosclerosis* 215(1):110–115. <https://doi.org/10.1016/j.atherosclerosis.2010.12.006>
23. Sacks HS, Fain JN (2007) Human epicardial adipose tissue: a review. *Am Heart J* 153(6):907–917. <https://doi.org/10.1016/j.ahj.2007.03.019>
24. Tanaka K, Sata M (2018) Roles of perivascular adipose tissue in the pathogenesis of atherosclerosis. *Front Physiol* 9:3. <https://doi.org/10.3389/fphys.2018.00003>
25. Hirata Y, Tabata M, Kurobe H, Motoki T, Akaike M et al (2011) Coronary atherosclerosis is associated with macrophage polarization in epicardial adipose tissue. *J Am Coll Cardiol* 58(3):248–255. <https://doi.org/10.1016/j.jacc.2011.01.048>
26. New SE, Aikawa E (2011) Molecular imaging insights into early inflammatory stages of arterial and aortic valve calcification. *Circ Res* 108(11):1381–1391. <https://doi.org/10.1161/circresaha.110.234146>
27. Tintut Y, Patel J, Parhami F, Demer LL (2000) Tumor necrosis factor- α promotes in vitro calcification of vascular cells via the cAMP pathway. *Circulation* 102(21):2636–2642. <https://doi.org/10.1161/01.cir.102.21.2636>
28. Kataoka Y, Wolski K, Uno K, Puri R, Tuzcu EM et al (2012) Spotty calcification as a marker of accelerated progression of coronary atherosclerosis: insights from serial intravascular ultrasound. *J Am Coll Cardiol* 59(18):1592–1597. <https://doi.org/10.1016/j.jacc.2012.03.012>
29. Stone GW, Maehara A, Lansky AJ, de Bruyne B, Cristea E et al (2011) A Prospective natural-history study of coronary atherosclerosis. *N Engl J Med* 364(3):226–235. <https://doi.org/10.1056/NEJMoa1002358>
30. Kataoka Y, Wolski K, Balog C, Uno K, Puri R et al (2014) Progression of coronary atherosclerosis in stable patients with ultrasonic features of high-risk plaques. *Eur Heart J Cardiovasc Imaging* 15(9):1035–1041. <https://doi.org/10.1093/ehjci/jeu065>
31. Ridker PM, Everett BM, Thuren T, MacFadyen JG, Chang WH et al (2017) Antiinflammatory therapy with canakinumab for atherosclerotic disease. *N Engl J Med* 377(12):1119–1131. <https://doi.org/10.1056/NEJMoa1707914>
32. Tardif JC, Kouz S, Waters DD, Bertrand OF, Diaz R et al (2019) Efficacy and safety of low-dose colchicine after myocardial infarction. *N Engl J Med* 381(26):2497–2505. <https://doi.org/10.1056/NEJMoa1912388>

Publisher's Note Springer Nature remains neutral with regard to jurisdictional claims in published maps and institutional affiliations.